

Branching Fraction Measurements of the Decays $B \rightarrow \eta_c K$, where $\eta_c \rightarrow K \bar{K} \pi$ and $\eta_c \rightarrow 4K$

The *BABAR* Collaboration

Abstract

In this report, we present the observation of the exclusive decays $B^0 \rightarrow \eta_c K^0$ and $B^+ \rightarrow \eta_c K^+$, and the measurement of the related branching fractions. Using a sample of $22.7 \times 10^6 \Upsilon(4S) \rightarrow B \bar{B}$ decays collected with the *BABAR* detector at the SLAC PEP-II asymmetric *B* Factory during 1999-2000, we have observed statistically significant signals in the $\eta_c \rightarrow K_S^0 K^\pm \pi^\mp$ and $K^+ K^- \pi^0$ channels and set upper limits in the $\eta_c \rightarrow K^+ K^- K^+ K^-$ channels. All the results presented are preliminary.

We have measured

$$\begin{aligned} \mathcal{B}(B^+ \rightarrow \eta_c K^+) &= (1.50 \pm 0.19 \pm 0.15 \pm 0.46) \times 10^{-3} \\ \mathcal{B}(B^0 \rightarrow \eta_c K^0) &= (1.06 \pm 0.28 \pm 0.11 \pm 0.33) \times 10^{-3} \end{aligned}$$

where the first error is statistical, the second systematic and the last due to the uncertainty on the world average $\eta_c \rightarrow K \bar{K} \pi$ branching fraction.

The BABAR Collaboration,

B. Aubert, D. Boutigny, J.-M. Gaillard, A. Hicheur, Y. Karyotakis, J. P. Lees, P. Robbe, V. Tisserand,
A. Zghiche

Laboratoire de Physique des Particules, F-74941 Annecy-le-Vieux, France

A. Palano, A. Pompili

Università di Bari, Dipartimento di Fisica and INFN, I-70126 Bari, Italy

G. P. Chen, J. C. Chen, N. D. Qi, G. Rong, P. Wang, Y. S. Zhu

Institute of High Energy Physics, Beijing 100039, China

G. Eigen, I. Ofte, B. Stugu

University of Bergen, Inst. of Physics, N-5007 Bergen, Norway

G. S. Abrams, A. W. Borgland, A. B. Breon, D. N. Brown, J. Button-Shafer, R. N. Cahn, E. Charles,
M. S. Gill, A. V. Gritsan, Y. Groysman, R. G. Jacobsen, R. W. Kadel, J. Kadyk, L. T. Kerth,
Yu. G. Kolomensky, J. F. Kral, C. LeClerc, M. E. Levi, G. Lynch, L. M. Mir, P. J. Oddone, M. Pripstein,
N. A. Roe, A. Romosan, M. T. Ronan, V. G. Shelkov, A. V. Telnov, W. A. Wenzel

Lawrence Berkeley National Laboratory and University of California, Berkeley, CA 94720, USA

T. J. Harrison, C. M. Hawkes, D. J. Knowles, S. W. O'Neale, R. C. Penny, A. T. Watson, N. K. Watson

University of Birmingham, Birmingham, B15 2TT, United Kingdom

T. Deppermann, K. Goetzen, H. Koch, B. Lewandowski, K. Peters, H. Schmuecker, M. Steinke

Ruhr Universität Bochum, Institut für Experimentalphysik 1, D-44780 Bochum, Germany

N. R. Barlow, W. Bhimji, N. Chevalier, P. J. Clark, W. N. Cottingham, B. Foster, C. Mackay, F. F. Wilson

University of Bristol, Bristol BS8 1TL, United Kingdom

K. Abe, C. Hearty, T. S. Mattison, J. A. McKenna, D. Thiessen

University of British Columbia, Vancouver, BC, Canada V6T 1Z1

S. Jolly, A. K. McKemey

Brunel University, Uxbridge, Middlesex UB8 3PH, United Kingdom

V. E. Blinov, A. D. Bukin, D. A. Bukin, A. R. Buzykaev, V. B. Golubev, V. N. Ivanchenko, A. A. Korol,
E. A. Kravchenko, A. P. Onuchin, S. I. Serednyakov, Yu. I. Skovpen, A. N. Yushkov

Budker Institute of Nuclear Physics, Novosibirsk 630090, Russia

D. Best, M. Chao, D. Kirkby, A. J. Lankford, M. Mandelkern, S. McMahon, D. P. Stoker

University of California at Irvine, Irvine, CA 92697, USA

K. Arisaka, C. Buchanan, S. Chun

University of California at Los Angeles, Los Angeles, CA 90024, USA

D. B. MacFarlane, S. Prell, Sh. Rahatlou, G. Raven, V. Sharma

University of California at San Diego, La Jolla, CA 92093, USA

C. Campagnari, B. Dahmes, P. A. Hart, N. Kuznetsova, S. L. Levy, O. Long, A. Lu, M. A. Mazur,
J. D. Richman, W. Verkerke

University of California at Santa Barbara, Santa Barbara, CA 93106, USA

J. Beringer, A. M. Eisner, M. Grothe, C. A. Heusch, W. S. Lockman, T. Pulliam, T. Schalk, R. E. Schmitz,
B. A. Schumm, A. Seiden, M. Turri, W. Walkowiak, D. C. Williams, M. G. Wilson

University of California at Santa Cruz, Institute for Particle Physics, Santa Cruz, CA 95064, USA

E. Chen, G. P. Dubois-Felsmann, A. Dvoretzskii, D. G. Hitlin, S. Metzler, J. Oyang, F. C. Porter, A. Ryd,
A. Samuel, S. Yang, R. Y. Zhu

California Institute of Technology, Pasadena, CA 91125, USA

S. Jayatilke, G. Mancinelli, B. T. Meadows, M. D. Sokoloff

University of Cincinnati, Cincinnati, OH 45221, USA

T. Barillari, P. Bloom, W. T. Ford, U. Nauenberg, A. Olivas, P. Rankin, J. Roy, J. G. Smith, W. C. van
Hoek, L. Zhang

University of Colorado, Boulder, CO 80309, USA

J. Blouw, J. L. Harton, M. Krishnamurthy, A. Soffer, W. H. Toki, R. J. Wilson, J. Zhang

Colorado State University, Fort Collins, CO 80523, USA

T. Brandt, J. Brose, T. Colberg, M. Dickopp, R. S. Dubitzky, A. Hauke, E. Maly, R. Müller-Pfefferkorn,
S. Otto, K. R. Schubert, R. Schwierz, B. Spaan, L. Wilden

Technische Universität Dresden, Institut für Kern- und Teilchenphysik, D-01062 Dresden, Germany

D. Bernard, G. R. Bonneaud, F. Brochard, J. Cohen-Tanugi, S. Ferrag, S. T'Jampens, Ch. Thiebaux,
G. Vasileiadis, M. Verderi

Ecole Polytechnique, LLR, F-91128 Palaiseau, France

A. Anjomshoaa, R. Bernet, A. Khan, D. Lavin, F. Muheim, S. Playfer, J. E. Swain, J. Tinslay

University of Edinburgh, Edinburgh EH9 3JZ, United Kingdom

M. Falbo

Elon University, Elon, NC 27244-2010, USA

C. Borean, C. Bozzi, L. Piemontese

Università di Ferrara, Dipartimento di Fisica and INFN, I-44100 Ferrara, Italy

E. Treadwell

Florida A&M University, Tallahassee, FL 32307, USA

F. Anulli,¹ R. Baldini-Ferrolì, A. Calcaterra, R. de Sangro, D. Falciari, G. Finocchiaro, P. Patteri,
I. M. Peruzzi,² M. Piccolo, Y. Xie, A. Zallo

Laboratori Nazionali di Frascati dell'INFN, I-00044 Frascati, Italy

S. Bagnasco, A. Buzzo, R. Contri, G. Crosetti, M. Lo Vetere, M. Macri, M. R. Monge, S. Passaggio,
F. C. Pastore, C. Patrignani, E. Robutti, A. Santroni, S. Tosi

Università di Genova, Dipartimento di Fisica and INFN, I-16146 Genova, Italy

¹ Also with Università di Perugia, I-06100 Perugia, Italy

² Also with Università di Perugia, I-06100 Perugia, Italy

M. Morii

Harvard University, Cambridge, MA 02138, USA

R. Bartoldus, R. Hamilton, U. Mallik

University of Iowa, Iowa City, IA 52242, USA

J. Cochran, H. B. Crawley, J. Lamsa, W. T. Meyer, E. I. Rosenberg, J. Yi

Iowa State University, Ames, IA 50011-3160, USA

G. Grosdidier, A. Höcker, H. M. Lacker, S. Laplace, F. Le Diberder, V. Lepeltier, A. M. Lutz,
S. Plaszczynski, M. H. Schune, S. Trincaz-Duvoid, G. Wormser

Laboratoire de l'Accélérateur Linéaire, F-91898 Orsay, France

R. M. Bionta, V. Brigljević, D. J. Lange, M. Mugge, K. van Bibber, D. M. Wright

Lawrence Livermore National Laboratory, Livermore, CA 94550, USA

A. J. Bevan, J. R. Fry, E. Gabathuler, R. Gamet, M. George, M. Kay, D. J. Payne, R. J. Sloane,
C. Touramanis

University of Liverpool, Liverpool L69 3BX, United Kingdom

M. L. Aspinwall, D. A. Bowerman, P. D. Dauncey, U. Egede, I. Eschrich, G. W. Morton, J. A. Nash,
P. Sanders, D. Smith

University of London, Imperial College, London, SW7 2BW, United Kingdom

J. J. Back, G. Bellodi, P. Dixon, P. F. Harrison, R. J. L. Potter, H. W. Shorthouse, P. Strother, P. B. Vidal

Queen Mary, University of London, E1 4NS, United Kingdom

G. Cowan, S. George, M. G. Green, A. Kurup, C. E. Marker, T. R. McMahon, S. Ricciardi, F. Salvatore,
G. Vaitsas

University of London, Royal Holloway and Bedford New College, Egham, Surrey TW20 0EX, United Kingdom

D. Brown, C. L. Davis

University of Louisville, Louisville, KY 40292, USA

J. Allison, R. J. Barlow, J. T. Boyd, A. C. Forti, F. Jackson, G. D. Lafferty, N. Savvas, J. H. Weatherall,
J. C. Williams

University of Manchester, Manchester M13 9PL, United Kingdom

A. Farbin, A. Jawahery, V. Lillard, J. Olsen, D. A. Roberts, J. R. Schieck

University of Maryland, College Park, MD 20742, USA

G. Blaylock, C. Dallapiccola, K. T. Flood, S. S. Hertzbach, R. Kofler, V. B. Koptchev, T. B. Moore,
H. Staengle, S. Willocq

University of Massachusetts, Amherst, MA 01003, USA

B. Brau, R. Cowan, G. Sciolla, F. Taylor, R. K. Yamamoto

Massachusetts Institute of Technology, Laboratory for Nuclear Science, Cambridge, MA 02139, USA

M. Milek, P. M. Patel

McGill University, Montréal, QC, Canada H3A 2T8

F. Palombo, C. Vite

Università di Milano, Dipartimento di Fisica and INFN, I-20133 Milano, Italy

J. M. Bauer, L. Cremaldi, V. Eschenburg, R. Kroeger, J. Reidy, D. A. Sanders, D. J. Summers

University of Mississippi, University, MS 38677, USA

C. Hast, J. Y. Nief, P. Taras

Université de Montréal, Laboratoire René J. A. Lévesque, Montréal, QC, Canada H3C 3J7

H. Nicholson

Mount Holyoke College, South Hadley, MA 01075, USA

C. Cartaro, N. Cavallo,³ G. De Nardo, F. Fabozzi, C. Gatto, L. Lista, P. Paolucci, D. Piccolo, C. Sciacca

Università di Napoli Federico II, Dipartimento di Scienze Fisiche and INFN, I-80126, Napoli, Italy

J. M. LoSecco

University of Notre Dame, Notre Dame, IN 46556, USA

J. R. G. Alsmiller, T. A. Gabriel

Oak Ridge National Laboratory, Oak Ridge, TN 37831, USA

J. Brau, R. Frey, E. Grauges, M. Iwasaki, C. T. Potter, N. B. Sinev, D. Strom

University of Oregon, Eugene, OR 97403, USA

F. Colecchia, F. Dal Corso, A. Dorigo, F. Galeazzi, M. Margoni, M. Morandin, M. Posocco, M. Rotondo,
F. Simonetto, R. Stroili, E. Torassa, C. Voci

Università di Padova, Dipartimento di Fisica and INFN, I-35131 Padova, Italy

M. Benayoun, H. Briand, J. Chauveau, P. David, Ch. de la Vaissière, L. Del Buono, O. Hamon,
Ph. Leruste, J. Ocariz, M. Pivk, L. Roos, J. Stark

Universités Paris VI et VII, Lab de Physique Nucléaire H. E., F-75252 Paris, France

P. F. Manfredi, V. Re, V. Speziali

Università di Pavia, Dipartimento di Elettronica and INFN, I-27100 Pavia, Italy

E. D. Frank, L. Gladney, Q. H. Guo, J. Panetta

University of Pennsylvania, Philadelphia, PA 19104, USA

C. Angelini, G. Batignani, S. Bettarini, M. Bondioli, F. Bucci, E. Campagna, M. Carpinelli, F. Forti,
M. A. Giorgi, A. Lusiani, G. Marchiori, F. Martinez-Vidal, M. Morganti, N. Neri, E. Paoloni, M. Rama,
G. Rizzo, F. Sandrelli, G. Simi, G. Triggiani, J. Walsh

Università di Pisa, Scuola Normale Superiore and INFN, I-56010 Pisa, Italy

M. Haire, D. Judd, K. Paick, L. Turnbull, D. E. Wagoner

Prairie View A&M University, Prairie View, TX 77446, USA

J. Albert, P. Elmer, C. Lu, V. Miftakov, S. F. Schaffner, A. J. S. Smith, A. Tumanov, E. W. Varnes

Princeton University, Princeton, NJ 08544, USA

³ Also with Università della Basilicata, I-85100 Potenza, Italy

F. Bellini, G. Cavoto, D. del Re, R. Faccini,⁴ F. Ferrarotto, F. Ferroni, M. A. Mazzoni, S. Morganti,
G. Piredda, M. Serra, C. Voena

Università di Roma La Sapienza, Dipartimento di Fisica and INFN, I-00185 Roma, Italy

S. Christ, R. Waldi

Universität Rostock, D-18051 Rostock, Germany

T. Adye, N. De Groot, B. Franek, N. I. Geddes, G. P. Gopal, S. M. Xella

Rutherford Appleton Laboratory, Chilton, Didcot, Oxon, OX11 0QX, United Kingdom

R. Aleksan, S. Emery, A. Gaidot, S. F. Ganzhur, P.-F. Giraud, G. Hamel de Monchenault, W. Kozanecki,
M. Langer, G. W. London, B. Mayer, B. Serfass, G. Vasseur, Ch. Yèche, M. Zito

DAPNIA, Commissariat à l'Energie Atomique/Saclay, F-91191 Gif-sur-Yvette, France

M. V. Purohit, A. W. Weidemann, F. X. Yumiceva

University of South Carolina, Columbia, SC 29208, USA

I. Adam, D. Aston, N. Berger, A. M. Boyarski, G. Calderini, M. R. Convery, D. P. Coupal, D. Dong,
J. Dorfan, W. Dunwoodie, R. C. Field, T. Glanzman, S. J. Gowdy, T. Haas, T. Hadig, V. Halyo, T. Himel,
T. Hryn'ova, M. E. Huffer, W. R. Innes, C. P. Jessop, M. H. Kelsey, P. Kim, M. L. Kocian,
U. Langenegger, D. W. G. S. Leith, S. Luitz, V. Luth, H. L. Lynch, H. Marsiske, S. Menke, R. Messner,
D. R. Muller, C. P. O'Grady, V. E. Ozcan, A. Perazzo, M. Perl, S. Petrak, H. Quinn, B. N. Ratcliff,
S. H. Robertson, A. Roodman, A. A. Salnikov, T. Schietinger, R. H. Schindler, J. Schwiening, A. Snyder,
A. Soha, S. M. Spanier, J. Stelzer, D. Su, M. K. Sullivan, H. A. Tanaka, J. Va'vra, S. R. Wagner,
M. Weaver, A. J. R. Weinstein, W. J. Wisniewski, D. H. Wright, C. C. Young

Stanford Linear Accelerator Center, Stanford, CA 94309, USA

P. R. Burchat, C. H. Cheng, T. I. Meyer, C. Roat

Stanford University, Stanford, CA 94305-4060, USA

R. Henderson

TRIUMF, Vancouver, BC, Canada V6T 2A3

W. Bugg, H. Cohn

University of Tennessee, Knoxville, TN 37996, USA

J. M. Izen, I. Kitayama, X. C. Lou

University of Texas at Dallas, Richardson, TX 75083, USA

F. Bianchi, M. Bona, D. Gamba

Università di Torino, Dipartimento di Fisica Sperimentale and INFN, I-10125 Torino, Italy

L. Bosisio, G. Della Ricca, S. Dittongo, L. Lanceri, P. Poropat, L. Vitale, G. Vuagnin

Università di Trieste, Dipartimento di Fisica and INFN, I-34127 Trieste, Italy

R. S. Panvini

Vanderbilt University, Nashville, TN 37235, USA

⁴ Also with University of California at San Diego, La Jolla, CA 92093, USA

C. M. Brown, P. D. Jackson, R. Kowalewski, J. M. Roney
University of Victoria, Victoria, BC, Canada V8W 3P6

H. R. Band, S. Dasu, M. Datta, A. M. Eichenbaum, H. Hu, J. R. Johnson, R. Liu, F. Di Lodovico, Y. Pan,
R. Prepost, I. J. Scott, S. J. Sekula, J. H. von Wimmersperg-Toeller, S. L. Wu, Z. Yu
University of Wisconsin, Madison, WI 53706, USA

T. M. B. Kordich, H. Neal
Yale University, New Haven, CT 06511, USA

1 Introduction

We present the measurement of the branching fractions of the exclusive decays¹ $B^0 \rightarrow \eta_c K^0$ and $B^+ \rightarrow \eta_c K^+$, with η_c decaying into $K_S^0 K^\pm \pi^\mp$, $K^+ K^- \pi^0$, and $K^+ K^- K^+ K^-$ ($K_S^0 \rightarrow \pi^+ \pi^-$ and $\pi^0 \rightarrow \gamma\gamma$). The η_c is a $c\bar{c}$ meson with $I^G(J^{PC}) = 0^+(0^{-+})$. The decay $B^0 \rightarrow \eta_c K^0$ proceeds through the same $b \rightarrow c\bar{c} s$ color-suppressed quark diagram as the “golden” mode, $B^0 \rightarrow J/\psi K^0$, used to measure the CP -violating parameter $\sin 2\beta$ with negligible theoretical uncertainty [1]. Up to now, experimental information on B decays into η_c has been sparse [2, 3].

The ratio of the decay rates for the exclusive charmonium decays

$$R_K \equiv \Gamma(B \rightarrow \eta_c K) / \Gamma(B \rightarrow J/\psi K) \quad (1)$$

has been calculated with different dynamical assumptions [4]–[8] including factorization². The ratio is used since one expects that the corrections to the heavy quark limit, due to the relatively light s -quark, are likely to cancel. This leads to the following predictions for R_K : 1.6 ± 0.2 [4], 1.64 ± 0.55 [5], $1.8 \sim 2.3$ [6], 0.94 ± 0.25 [7], $1.0 \sim 1.3$ [8].

2 The *BABAR* detector and dataset

The data used in this analysis are obtained with the *BABAR* detector at the PEP-II asymmetric e^+e^- storage ring. The *BABAR* detector is described elsewhere [10]. The 1.5 T superconducting solenoidal magnet, whose cylindrical volume is ≈ 1.4 m in radius and ≈ 3 m long, contains a charged-particle tracking system, a Cherenkov detector (DIRC) dedicated to charged particle identification and an electromagnetic calorimeter. The segmented iron flux return, including endcaps, provides identification of muons and K_L^0 . In addition, the end of the cylindrical volume in the e^- direction is instrumented with an electromagnetic calorimeter. The tracking system consists of a 5-layer double-sided silicon vertex tracker and a 40-layer drift chamber filled with a gas mixture of helium and isobutane. The calorimeter consists of 6580 CsI(Tl) crystals. The flux return is instrumented with resistive plate chambers.

We have used data corresponding to 20.7 fb^{-1} of integrated luminosity collected at the $\Upsilon(4S)$ resonance (“on-resonance”), and 2.1 fb^{-1} recorded (“off-resonance”) about 40 MeV lower in energy in the $\Upsilon(4S)$ rest frame (“CM”), between October 1999 and October 2000. The asymmetric collisions produce a boost in the e^- direction, with $\beta\gamma = 0.55$ in on-resonance running.

¹Throughout this paper, whenever a mode is given, the charge conjugate (c.c.) is also implied.

²We note that we have measured a departure from the factorization hypothesis [9] in another $b \rightarrow c\bar{c} s$ color-suppressed mode, $B \rightarrow J/\psi K^*$, wherein we have made a polarization measurement, more sensitive than a measurement of R_K to the existence of a factorization-violating term.

3 Analysis method

A blind analysis is performed in which all selections are chosen to maximize $N_S/\sqrt{N_S+N_B}$ using simulated or off-resonance data, or sidebands in on-resonance data. $N_S(N_B)$ is the number of expected signal (background) events after all selection criteria have been applied.

Event selection designed to enhance the number of B decays requires four or more charged tracks, the sum of all charged and neutral energies to be above 2 GeV, the sum of all the charged momenta to be above 1 GeV/ c , and the normalized second Fox-Wolfram moment [11] to be less than 0.6. In addition, at least one neutral or charged kaon candidate is required to have a momentum in the $\Upsilon(4S)$ rest frame consistent with the two-body decay $B \rightarrow \eta_c K$.

B^0 or B^\pm candidates are formed from an η_c candidate and a “fast” kaon, either a charged kaon or a $K_S^0 \rightarrow \pi^+\pi^-$. The η_c candidates correspond to three different topologies: two charged tracks with either $K_S^0 \rightarrow \pi^+\pi^-$ or $\pi^0 \rightarrow \gamma\gamma$, or four charged tracks. The B decay vertex is calculated using the charged η_c daughters, and the fast kaon if charged.

We require that all charged tracks be within $0.35 < \theta < 2.54$ to obtain well-reconstructed tracks, where θ is the polar angle with respect to the e^- direction. An important requirement of our analysis is that charged kaon candidates from the $B \rightarrow \eta_c K$ decay are identified by the DIRC and/or by measurements of ionization energy loss dE/dx in the drift chamber and silicon tracker. The momentum of each kaon from η_c decay is required to be greater than 250 MeV/ c .

The K_S^0 particles can arise from η_c or B decays. In the following, the number in parentheses corresponds to the latter K_S^0 . The $K_S^0 \rightarrow \pi^+\pi^-$ candidates are required to have a reconstructed invariant mass within 12.5 (10) MeV/ c^2 of the nominal, i.e. world average, value [12]. Furthermore, the cosine of the opening angle between the flight direction and the momentum vector of the K_S^0 candidate is required to be greater than 0.990 (0.9995), and the flight distance from the B vertex greater than 2 (3) times its error.

The $\pi^0 \rightarrow \gamma\gamma$ candidates are formed from pairs of photons detected in the calorimeter with a reconstructed invariant mass within 15 MeV/ c^2 of the nominal value. We require that the cosine of the decay angle in the π^0 rest frame be less than 0.82 to avoid accidental combinations involving very soft photons. In addition, the electromagnetic showers are required to have moments of the lateral energy deposition [15] between 0.01 and 0.55. The lower energy photon has a minimum energy of 130 MeV while the minimum value for the higher energy photon is 270 MeV.

A Fisher discriminant is used to suppress continuum backgrounds. The Fisher variable is defined as a linear combination of eighteen variables, including the energies between each of nine cones relative to the η_c direction in the CM [14]. The most important variables are the normalized second Fox-Wolfram moment and the event thrust, constructed with all charged tracks and neutral clusters in the event. The Fisher discriminant is trained on signal, $u\bar{u}$, $d\bar{d}$, $s\bar{s}$, and $c\bar{c}$ simulated events, and tested on off-resonance data. The requirements on the Fisher discriminant depends on the decay mode.

The charmonium mass region is defined by $2.74 < m_X < 3.22$ GeV/ c^2 . After all selection criteria, the weighted double-Gaussian mass resolutions are 10, 12, and 26 MeV/ c^2 for the $K_S^0 K^\pm \pi^\mp$, $K^+ K^- K^+ K^-$ and $K^+ K^- \pi^0$ channels, respectively, as obtained from a simulation. The η_c signal region varies between ± 55 MeV/ c^2 and ± 70 MeV/ c^2 relative to the nominal η_c mass (2979.8 MeV/ c^2), depending on the η_c decay mode.

The total energy of the e^+e^- system in the $\Upsilon(4S)$ CM and laboratory frames are denoted by \sqrt{s} and E_o , respectively. In the e^+e^- laboratory frame, the candidate energy is defined as $E_B = (s/2 + \mathbf{p}_o \cdot \mathbf{p}_B)/E_o$, where \mathbf{p}_o and \mathbf{p}_B are the momentum vectors of the e^+e^- system and

the B candidate, respectively [10]. The analysis region is defined by a rectangular area in the ΔE - m_{ES} plane where ΔE is the difference between the energy of the B candidate in the CM frame and $\sqrt{s}/2$, and m_{ES} is the beam-energy substituted mass, $\sqrt{E_B^2 - p_B^2}$. For events with multiple candidates, the one with the smallest $|\Delta E|$ is retained; this choice affects only a small fraction of events, from 3.4% to 12.4% in the analysis region.

The limits of the analysis region are defined by $5.1 < m_{\text{ES}} < 5.29$ GeV/ c^2 and $|\Delta E| < 0.25$ GeV. According to the full detector simulation based on GEANT3 [13], depending on the η_c decay mode, the signal is Gaussian-distributed in ΔE with a mean near zero and a resolution between 15 and 30 MeV, while it is Gaussian-distributed in m_{ES} with a mean near the B mass and a resolution around 2.5 MeV/ c^2 . The ΔE resolution depends on the η_c decay mode, best for $K_S^0 K^\pm \pi^\mp$ and worst for $K^+ K^- \pi^0$. Note that the ΔE distribution in data is not centered at zero but rather at about -10 MeV; the window is shifted accordingly, leading to a contribution to the overall systematic error. The shifted- $|\Delta E|, |m_{\text{ES}} - m_B^{\text{nominal}}|$ signal region is < 30 MeV, < 7 MeV/ c^2 for the tightest ($K_S^0 K^\pm \pi^\mp$) case and < 70 MeV, < 9 MeV/ c^2 for the loosest ($K^+ K^- \pi^0$) case.

4 Observation of exclusive η_c signals

Figure 1 displays the mass distribution of the charmonium system in the $(\Delta E, m_{\text{ES}})$ signal region for the $K_S^0 K^\pm \pi^\mp$ channel, using B^+ candidates after subtraction of the combinatorial background. We see clear η_c and J/ψ peaks where we have indicated the η_c mass selection excluding the J/ψ region. The representative curves are fits of three contributions: flat background, J/ψ peak, and η_c peak with two different widths. The J/ψ peak is represented by a Gaussian with mean constrained at the nominal J/ψ mass and a 12 MeV/ c^2 resolution. The η_c mass peak is represented by a Breit-Wigner distribution convoluted with the same Gaussian. The mean of the Breit-Wigner distribution is fixed at the nominal η_c mass and the width³, either to the world average or to the CLEO measurement [16]. Since we cannot yet distinguish among the various measurements, we have used for the η_c width the average value 16.7 ± 6.0 MeV/ c^2 ; the efficiency depends on the width central value and the systematic error on its error.

In Figure 2 we display the analysis region for the B^+ and B^0 ($\eta_c \rightarrow K_S^0 K^\pm \pi^\mp$) channels as examples. Clear accumulations in the $(\Delta E, m_{\text{ES}})$ signal region are apparent. Figures 3 and 4 display projections of the analysis region for the different η_c channels. The combinatorial background shape is parametrized by a linear function in ΔE and a threshold function [19] in m_{ES} with a fixed endpoint given by the average beam energy.

In addition to the combinatorial background, a background that peaks in the $(\Delta E, m_{\text{ES}})$ signal region can arise from cross-feed from other η_c decay modes, from partial reconstruction and/or incorrect particle identification, or from B decays into the same detected particles without an intermediate η_c decay (exact matches). After study, the first two sources are found to be negligible. A quantitative evaluation of the exact matches for each mode is made using data by studying the η_c mass sidebands for events in the $(\Delta E, m_{\text{ES}})$ signal region, after subtracting the combinatorial background as a function of mass. The peaking background is consistent with zero for all modes except possibly for the $K_S^0 K^\pm \pi^\mp$ mode, see the flat background in Figure 1.

The raw yield and expected backgrounds in the $(\Delta E, m_{\text{ES}})$ signal region, and the probability that the background fluctuates to the observed yield are given in Table 1. In order to ensure the

³ The world average width is $13.2_{-3.2}^{+3.8}$ MeV/ c^2 while more recent results give $27.0 \pm 5.8 \pm 1.4$ MeV/ c^2 [16], $11.0 \pm 8.1 \pm 4.1$ MeV/ c^2 [17] and $21.1_{-6.2}^{+6.9}$ MeV/ c^2 [18]

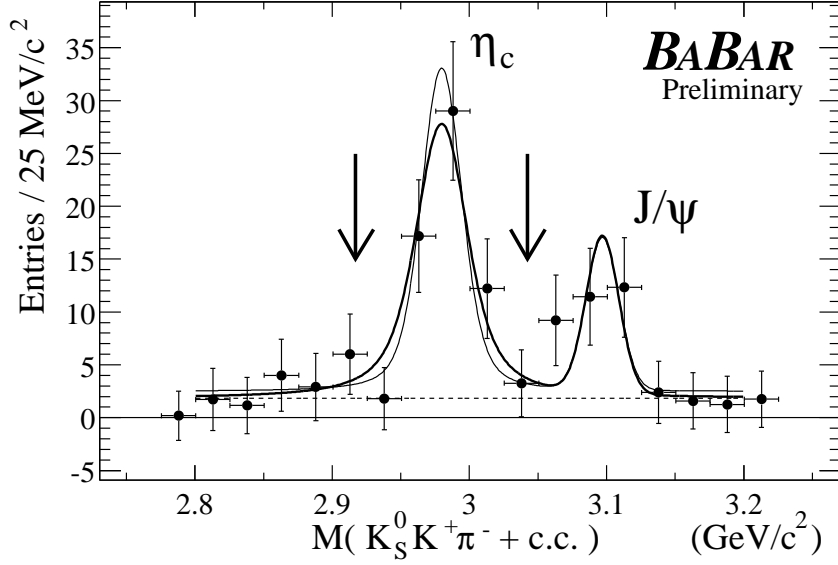


Figure 1: $K_S^0 K^\pm \pi^\mp$ mass for B^+ candidates in the $(\Delta E, m_{ES})$ signal region after subtraction of the combinatorial background. The fits are described in the text. The remaining flat background is that due to the peaking background; see text. The “thick” curve corresponds to the CLEO η_c width while the “thin” curve corresponds to the world average.

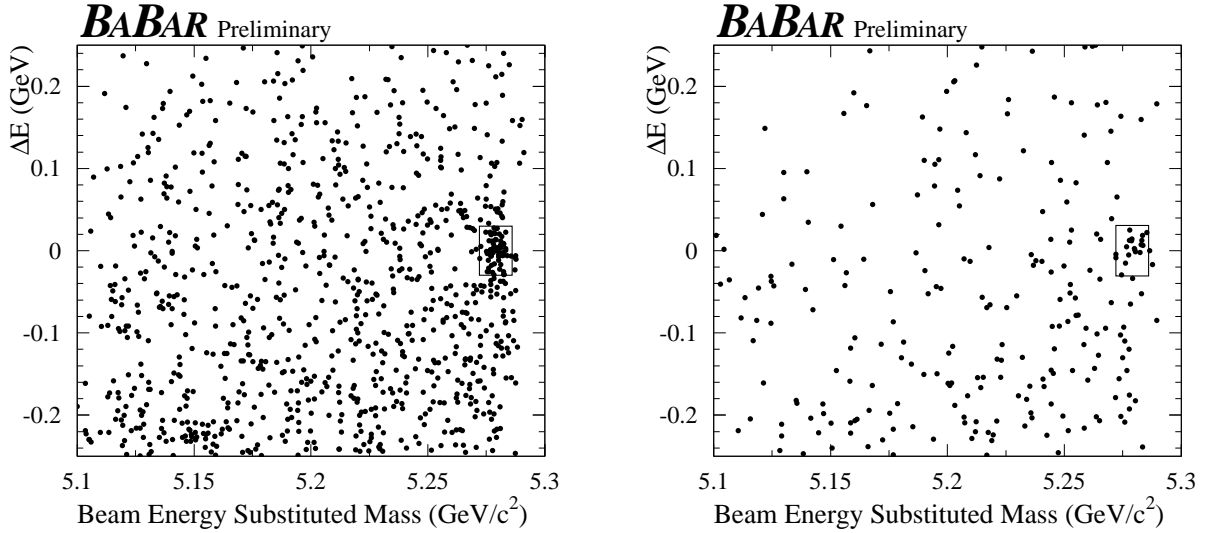


Figure 2: ΔE vs. m_{ES} for candidate $B^+ \rightarrow \eta_c K^+$ events (on left) and $B^0 \rightarrow \eta_c K_S^0$ events (on right), with $\eta_c \rightarrow K_S^0 K^\pm \pi^\mp$. The $(\Delta E, m_{ES})$ signal region is indicated. All selection criteria have been applied except for the signal region requirements.

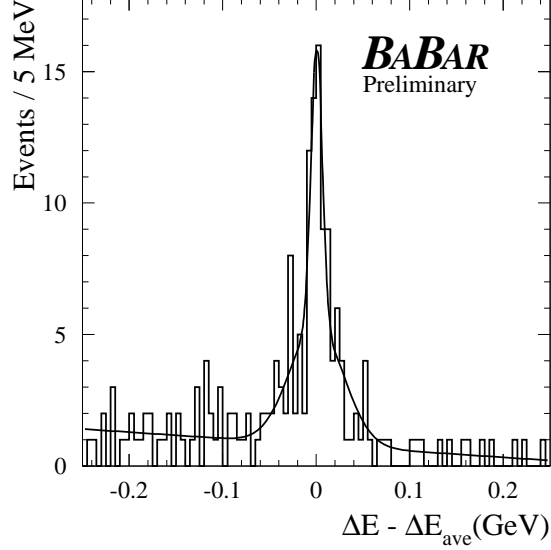


Figure 3: The ΔE distribution relative to its mean in the m_{ES} signal band for combined $B^+ \rightarrow \eta_c K^+$ and $B^0 \rightarrow \eta_c K_S^0$ candidates with $\eta_c \rightarrow K_S^0 K^\pm \pi^\mp$, fitted to a double Gaussian with common mean on top of a linear background. The weighted average resolution is $16.3 \text{ MeV}/c^2$. The narrower Gaussian represents 71% of the area of the double Gaussian; its resolution is $5.9 \text{ MeV}/c^2$. All selection criteria have been applied except that for ΔE .

statistical independence of the signal and background measurements, the combinatorial background is estimated here by the extrapolation into the m_{ES} signal band of the threshold function fitted in the ΔE signal band below the m_{ES} signal band ($m_{ES} < 5.27 \text{ GeV}/c^2$). Because of the low statistics in the B^0 channels, the shape parameter of the background function is fixed to that fitted in the corresponding B^+ channel.

Table 1: Raw yield, extrapolated combinatorial (see text) and peaking backgrounds in the $(\Delta E, m_{ES})$ signal region, and Poisson probability that the combined background fluctuates to the number of events found in the signal region (called “ Prob_{fluct} ”). Due to the limited data sample, the fitted combinatorial background estimate for B^0 ($\eta_c \rightarrow K^+ K^- K^+ K^-$) comes from the ΔE sidebands.

mode	Yield	Fitted combinatorial background	Peaking background	Prob_{fluct}
B^+ ($\eta_c \rightarrow K_S^0 K^\pm \pi^\mp$)	72	6.08 ± 1.39	6.12 ± 2.61	2×10^{-16}
B^+ ($\eta_c \rightarrow K^+ K^- \pi^0$)	25	2.92 ± 0.92	0.58 ± 0.58	3×10^{-15}
B^+ ($\eta_c \rightarrow K^+ K^- K^+ K^-$)	17	7.41 ± 1.78	1.72 ± 2.75	2×10^{-3}
B^0 ($\eta_c \rightarrow K_S^0 K^\pm \pi^\mp$)	19	1.18 ± 0.38	1.48 ± 1.08	3×10^{-13}
B^0 ($\eta_c \rightarrow K^+ K^- \pi^0$)	8	1.73 ± 0.38	0	4×10^{-4}
B^0 ($\eta_c \rightarrow K^+ K^- K^+ K^-$)	1	1.01 ± 0.25	-	-

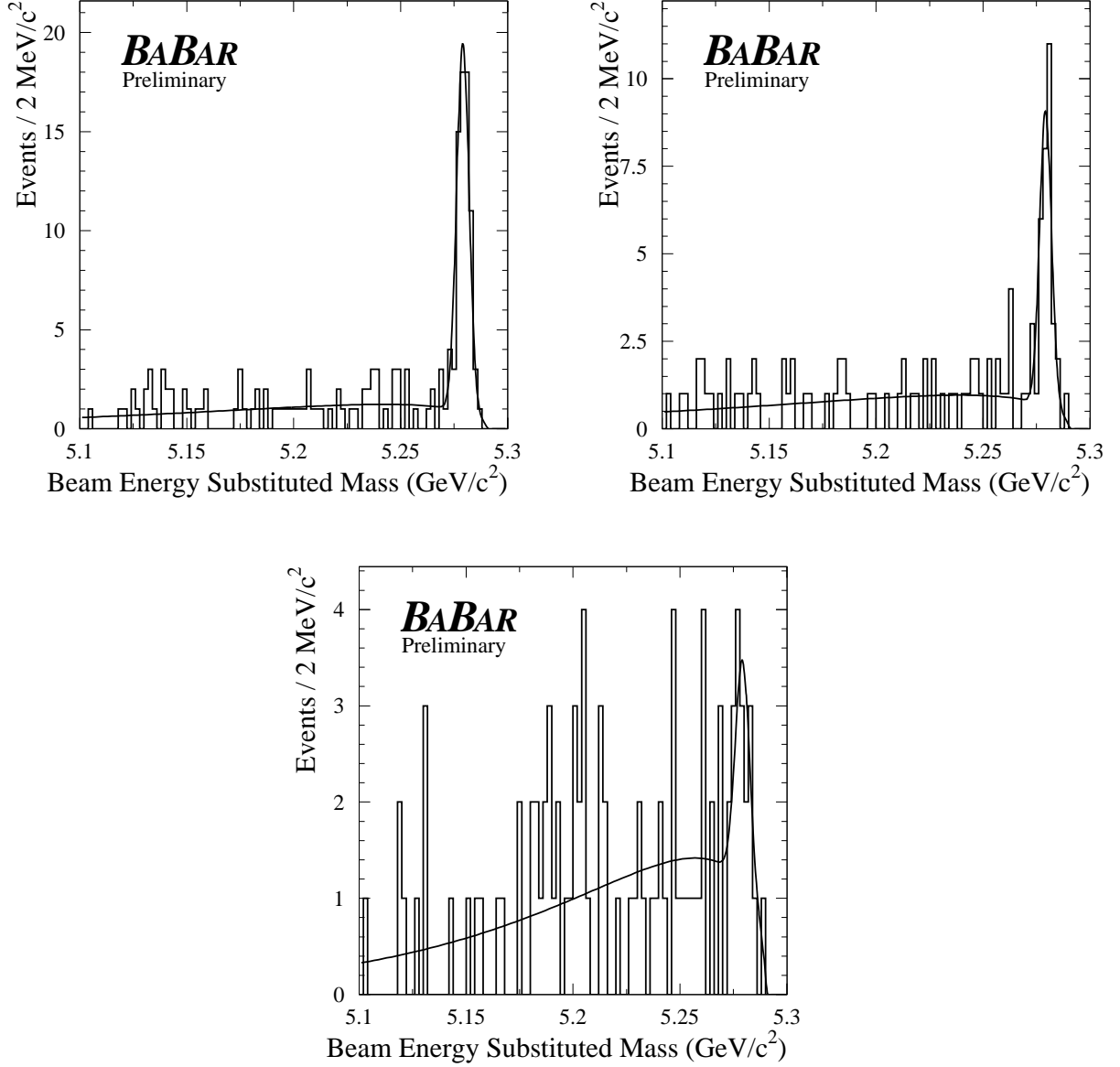


Figure 4: m_{ES} distributions in the ΔE signal band for candidate η_c decays: $K_s^0 K^\pm \pi^\mp$ (top left), $K^+ K^- \pi^0$ (top right), and $K^+ K^- K^+ K^-$ (bottom). All plots use combined B^+ and B^0 data and are fitted, using a binned likelihood method, to the sum of a Gaussian signal, with an average resolution of $2.9 \text{ MeV}/c^2$, and a threshold background function [19]. All selection criteria have been applied except that m_{ES} .

5 Branching fraction determination

The measured B^+ or B^0 branching fraction (\mathcal{B}) is given by

$$\mathcal{B} = \frac{N_{yield}}{N_{B\bar{B}} \times \epsilon}, \quad (2)$$

where N_{yield} is the net yield in the $(\Delta E, m_{ES})$ signal region, extracted from fits to the m_{ES} distributions in the ΔE signal region (Figure 4), and corrected for the peaking background contributions listed in Table 1; ϵ is the signal efficiency determined by applying the same analysis chain to signal Monte Carlo (MC) samples and correcting for data-MC differences; and $N_{B\bar{B}}$ is the number of produced $B\bar{B}$ pairs, $(22.73 \pm 0.36) \times 10^6$, determined by a comparison of the rate of multihadron events taken on-resonance to that off-resonance.

5.1 Determination of signal efficiency

The efficiency for reconstructing $B \rightarrow \eta_c K$ candidates for each η_c decay mode is given by the fraction of generated signal events that are reconstructed in the appropriate mode. We have compared simulations with real data, using for example $\tau^+\tau^-$ and $D^{*\pm}$ control samples. There are small differences in reconstruction efficiency for charged particles, K_S^0 and π^0 mesons, vertexing efficiency, resolution and absolute scale of charged particle momentum and photon energies, and charged kaon identification and pion misidentification probabilities. These effects have been measured and corrected. The resulting efficiencies are given in the first line of Table 2.

Table 2: Relative systematic errors on efficiency. All values are expressed in percentage relative to the efficiency, which is given in the first line as a fraction. The last line gives the total relative systematic error obtained as a sum in quadrature of the individual contributions. The 1.6% error from the determination of the number of $B\bar{B}$ events, common to all modes, is not listed but is included in the total as is the statistical error on the efficiency determination.

η_c decay	$B^0 \rightarrow \eta_c K_S^0$ $K^+K^- K^+K^-$	$B^0 \rightarrow \eta_c K_S^0$ $K_S^0 K^\pm \pi^\mp$	$B^0 \rightarrow \eta_c K_S^0$ $K^+K^- \pi^0$	$B^+ \rightarrow \eta_c K^+$ $K^+K^- K^+K^-$	$B^+ \rightarrow \eta_c K^+$ $K_S^0 K^\pm \pi^\mp$	$B^+ \rightarrow \eta_c K^+$ $K^+K^- \pi^0$
Efficiency	0.111	0.148	0.0733	0.117	0.145	0.0635
Rel. stat. err.	0.004	0.003	0.0027	0.003	0.003	0.0017
Tracking eff.	9.5	7.7	5.8	7.8	6.2	4.4
K_S^0 eff. and cuts	5.9	12.2	5.3	-	6.8	-
γ eff. and π^0 cuts	-	-	3.5	-	-	3.5
Vertexing eff.	1.3	1.0	1.0	1.3	1.0	1.0
Kaon ident. eff.	10.5	2.9	5.6	14.1	6.5	9.2
Fisher cut eff.	2.3	2.2	4.0	1.1	2.9	4.0
η_c width uncert.	2.9	3.2	3.1	2.9	3.2	3.1
ΔE centroid shift	0.47	3.3	0.86	0.51	2.7	0.24
ΔE resolution	3.6	3.8	4.4	3.4	5.2	3.4
Σ	16.2	16.1	12.3	16.8	13.5	12.4

5.2 Determination of systematic errors

We have evaluated the systematic errors on the yield, B counting and efficiency determination. The systematic error on the yield comes from a comparison of the combinatorial background estimations from the ΔE side and signal bands while that on B counting comes principally from the uncertainty on the efficiency due to small differences between data and simulation.

Each of the efficiency corrections, as well as our knowledge of the η_c width, has a corresponding systematic uncertainty. In addition, each requirement in the analysis method has been studied to evaluate any systematic differences between simulation and data. The dominant systematic errors

on the signal efficiency are due to kaon identification, tracking efficiency, and K_S^0 reconstruction as can be seen in Table 2.

5.3 Results

Our results for the product of the branching fractions for each mode are listed below. We have used the nominal values for the $K_S^0 \rightarrow \pi^+\pi^-$ and $\pi^0 \rightarrow \gamma\gamma$ branching fractions. The $B \rightarrow \eta_c K$ branching-fraction determinations assume that the branching fraction of the $\Upsilon(4S)$ into $B\bar{B}$ is 100%, with an equal admixture of charged and neutral B final states, and similarly for K^0 relative to K_S^0 and K_L^0 .

$$\begin{aligned}
\mathcal{B}(B^+ \rightarrow \eta_c K^+) \mathcal{B}(\eta_c \rightarrow K^0 K^- \pi^+ + \text{c.c.}) &= (52.8 \pm 7.9 \pm 7.3) \times 10^{-6} \\
\mathcal{B}(B^+ \rightarrow \eta_c K^+) \mathcal{B}(\eta_c \rightarrow K^+ K^- \pi^0) &= (15.5 \pm 3.6 \pm 2.5) \times 10^{-6} \\
\mathcal{B}(B^+ \rightarrow \eta_c K^+) \mathcal{B}(\eta_c \rightarrow K^+ K^- K^+ K^-) &< 5.6 \times 10^{-6} \text{ (90\% CL)} \\
\mathcal{B}(B^0 \rightarrow \eta_c K^0) \mathcal{B}(\eta_c \rightarrow K^0 K^- \pi^+ + \text{c.c.}) &= (36.8 \pm 11.6 \pm 6.0) \times 10^{-6} \\
\mathcal{B}(B^0 \rightarrow \eta_c K^0) \mathcal{B}(\eta_c \rightarrow K^+ K^- \pi^0) &= (11.3 \pm 5.1 \pm 2.4) \times 10^{-6} \\
\mathcal{B}(B^0 \rightarrow \eta_c K^0) \mathcal{B}(\eta_c \rightarrow K^+ K^- K^+ K^-) &< 2.3 \times 10^{-6} \text{ (90\% CL)}
\end{aligned}$$

The first error is statistical and the second systematic. The central value for $\mathcal{B}(B^+ \rightarrow \eta_c K^+) \mathcal{B}(\eta_c \rightarrow K^+ K^- K^+ K^-)$ is 3.2×10^{-6} , while the two-sided 68% CL varies from 2.6×10^{-6} to 4.1×10^{-6} . No correction is made for any potential $\phi\phi$ contribution to the $K^+ K^- K^+ K^-$ channels.

The channels $\eta_c \rightarrow K_S^0 K^\pm \pi^\mp$ and $\eta_c \rightarrow K^+ K^- \pi^0$ are manifestations of the general decay $\eta_c \rightarrow K \bar{K} \pi$. From isospin symmetry, the corresponding rates are related by simple Clebsch-Gordon coefficients: $\mathcal{B}(\eta_c \rightarrow K^0 K^- \pi^+ + \text{c.c.}) = 2/3 \mathcal{B}(\eta_c \rightarrow K \bar{K} \pi)$ and $\mathcal{B}(\eta_c \rightarrow K^+ K^- \pi^0) = 1/6 \mathcal{B}(\eta_c \rightarrow K \bar{K} \pi)$. Therefore the ratio of branching fractions, $\mathcal{B}(\eta_c \rightarrow K^+ K^- \pi^0) / \mathcal{B}(\eta_c \rightarrow K^0 K^- \pi^+ + \text{c.c.})$, should be 0.25. Our measurements are consistent with this value for B^+ ($0.29 \pm 0.08 \pm 0.04$) and B^0 ($0.31 \pm 0.17 \pm 0.05$).

We therefore combine our two results, taking into account common systematic errors, to obtain the values for the general decay:

$$\begin{aligned}
\mathcal{B}(B^+ \rightarrow \eta_c K^+) \mathcal{B}(\eta_c \rightarrow K \bar{K} \pi) &= (82.5 \pm 10.4 \pm 8.3) \times 10^{-6} \\
\mathcal{B}(B^0 \rightarrow \eta_c K^0) \mathcal{B}(\eta_c \rightarrow K \bar{K} \pi) &= (58.1 \pm 15.2 \pm 6.3) \times 10^{-6}.
\end{aligned}$$

The first error is statistical and the second systematic. We deduce the branching fraction ratio from our measurements of the $K \bar{K} \pi$ channel: $\mathcal{B}(B^0 \rightarrow \eta_c K^0) / \mathcal{B}(B^+ \rightarrow \eta_c K^+) = 0.71 \pm 0.20 \pm 0.08$. We have not used the $\eta_c \rightarrow K^+ K^- K^+ K^-$ results since their statistical weight would be marginal.

Using the world average for the $\eta_c \rightarrow K \bar{K} \pi$ branching fraction, 0.055 ± 0.017 [12], our results become

$$\begin{aligned}
\mathcal{B}(B^+ \rightarrow \eta_c K^+) &= (1.50 \pm 0.19 \pm 0.15 \pm 0.46) \times 10^{-3} \\
\mathcal{B}(B^0 \rightarrow \eta_c K^0) &= (1.06 \pm 0.28 \pm 0.11 \pm 0.33) \times 10^{-3},
\end{aligned}$$

where the last error is due to the $\eta_c \rightarrow K \bar{K} \pi$ branching fraction. We have not used the $\eta_c \rightarrow K^+ K^- K^+ K^-$ results since the η_c branching fraction is not very well known. We compare these results to the exclusive branching fractions measured by CLEO [3]: $\mathcal{B}(B^+ \rightarrow \eta_c K^+) = (0.69_{-0.21}^{+0.26} \pm 0.08 \pm 0.20) \times 10^{-3}$ and $\mathcal{B}(B^0 \rightarrow \eta_c K^0) = (1.09_{-0.42}^{+0.55} \pm 0.12 \pm 0.31) \times 10^{-3}$. The third error is that due to the nominal $J/\psi \rightarrow \gamma \eta_c$ branching fraction. Assuming that the errors due to the nominal branching fractions cancel, our results differ by a factor 2.2 ± 0.9 for the B^+ channel, combining statistical and systematic errors in quadrature. The B^0 channel results are consistent.

To determine R_K , we have used our measurements [20] of the branching fractions, $\mathcal{B}(B^+ \rightarrow J/\psi K^+) = (10.1 \pm 0.3 \pm 0.5) \times 10^{-4}$ and $\mathcal{B}(B^0 \rightarrow J/\psi K^0) = (8.5 \pm 0.5 \pm 0.6) \times 10^{-4}$, taking into account common systematic errors, to obtain

$$\begin{aligned} R_K^+ &= \Gamma(B^+ \rightarrow \eta_c K^+)/\Gamma(B^+ \rightarrow J/\psi K^+) = 1.48 \pm 0.19 \pm 0.17 \pm 0.46 \\ R_K^0 &= \Gamma(B^0 \rightarrow \eta_c K^0)/\Gamma(B^0 \rightarrow J/\psi K^0) = 1.24 \pm 0.33 \pm 0.16 \pm 0.38 \end{aligned}$$

where the first error is statistical, the second systematic and the third due to the $\eta_c \rightarrow K\bar{K}\pi$ branching fraction. Our results agree with the theoretical predictions listed at the end of Section 1.

6 Acknowledgments

We are grateful for the extraordinary contributions of our PEP-II colleagues in achieving the excellent luminosity and machine conditions that have made this work possible. The success of this project also relies critically on the expertise and dedication of the computing organizations that support *BABAR*. The collaborating institutions wish to thank SLAC for its support and the kind hospitality extended to them. This work is supported by the US Department of Energy and National Science Foundation, the Natural Sciences and Engineering Research Council (Canada), Institute of High Energy Physics (China), the Commissariat à l’Energie Atomique and Institut National de Physique Nucléaire et de Physique des Particules (France), the Bundesministerium für Bildung und Forschung (Germany), the Istituto Nazionale di Fisica Nucleare (Italy), the Research Council of Norway, the Ministry of Science and Technology of the Russian Federation, and the Particle Physics and Astronomy Research Council (United Kingdom). Individuals have received support from the A. P. Sloan Foundation, the Research Corporation, and the Alexander von Humboldt Foundation.

References

- [1] *BABAR* Collaboration, B. Aubert *et al.*, Phys. Rev. Lett. **87**, 091801 (2001); Belle Collaboration, K. Abe *et al.*, Phys. Rev. Lett. **87**, 091802 (2001).
- [2] CLEO Collaboration, R. Balest *et al.*, Phys. Rev. D **52**, 2661 (1995).
- [3] CLEO Collaboration, K. W. Edwards *et al.*, Phys. Rev. Lett. **86**, 30 (2001).
- [4] M. R. Ahmady and R. R. Mendel, Z. Phys. C **65**, 263 (1995).
- [5] N. G. Deshpande and J. Trampetic, Phys. Lett. B **339**, 270 (1994).
- [6] M. Gourdin *et al.*, Phys. Rev. D **52**, 1597 (1995).
- [7] P. Colangelo *et al.*, Phys. Lett. B **352**, 134 (1995).
- [8] D. S. Hwang and G.-H. Kim, Z. Phys. C **76**, 107 (1997).
- [9] *BABAR* Collaboration, B. Aubert *et al.*, Phys. Rev. D **65**, 032001 (2002).
- [10] *BABAR* Collaboration, B. Aubert *et al.*, Nucl. Instr. and Methods A **479**, 1 (2002).

- [11] G. C. Fox and S. Wolfram, *Phys. Rev. Lett.* **41**, 1581 (1978).
- [12] Particle Data Group, D. E. Groom *et al.*, *Eur. Phys. Jour. C* **15**, 1 (2000).
- [13] “GEANT, Detector Description and Simulation Tool,” CERN Program Library Long Writeup W5013 (1994).
- [14] CLEO Collaboration, D. M. Asner *et al.*, *Phys. Rev. D* **53**, 1039 (1996).
- [15] A. Drescher *et al.*, *Nucl. Instr. and Methods A* **237**, 464 (1985).
- [16] CLEO Collaboration, G. Brandenburg *et al.*, *Phys. Rev. Lett.* **85**, 3095 (2000).
- [17] BES Collaboration, J. Z. Bai *et al.*, hep-ex/0002006 (2000).
- [18] E835 Collaboration, M. Ambrogiani *et al.*, *Nucl. Phys. A* **692**, 308 (2001).
- [19] ARGUS Collaboration, H. Albrecht *et al.*, *Z. Phys. C* **48**, 543 (1990).
- [20] *BABAR* Collaboration, B. Aubert *et al.*, *Phys. Rev. D* **65**, 032001 (2002).